

# Breathable hydrogel dressings containing natural antioxidants for management of skin disorders

Journal of Biomaterials Applications

2019, Vol. 33(9) 1265–1276

© The Author(s) 2019


Article reuse guidelines:

sagepub.com/journals-permissions

DOI: 10.1177/0885328218816526

journals.sagepub.com/home/jba



**Mattia Comotto<sup>1,2,3</sup>, Saghi Saghazadeh<sup>1,2</sup>, Sara Bagherifard<sup>1,2,4</sup>, Bahar Aliakbarian<sup>5</sup>, Mehdi Kazemzadeh-Narbat<sup>1,2</sup>, Fatemeh Sharifi<sup>1,2</sup>, Seyed Ali Mousavi Shaegh<sup>1,2,6</sup>, Elmira Arab-Tehrany<sup>7</sup>, Nasim Annabi<sup>1,2,8</sup>, Patrizia Perego<sup>3</sup>, Ali Khademhosseini<sup>1,2,9,10</sup> and Ali Tamayol<sup>1,2,11</sup>** 

## Abstract

Traditional wound dressings are not effective enough to regulate the moisture content and remove excessive exudate from the environment. Wet wound dressings formed from hydrogels such as alginate are widely used in clinical practice for treatment of skin disorders. Here, we functionalize alginate dressings with natural antioxidants such as curcumin and t-resveratrol to render them both anti-inflammatory and antibacterial. The hydrogel maintains excellent mechanical properties and oxygen permeability over time. The release rate of the compounds from the hydrogels is assessed and their impact on bacterial and cellular growth is evaluated. The antioxidant compounds act as bactericidal agents and improve cell viability. The optimal concentration of active compounds in the engineered alginate-based dressings is determined.

## Keywords

Hydrogels, wet wound dressings, alginate, curcumin, t-resveratrol

## Introduction

Skin disorders are common and affect millions of people worldwide. Chronic wounds are among the most challenging skin disorders that do not heal in an

<sup>9</sup>Center of Nanotechnology, Department of Physics, King Abdulaziz University, Jeddah, Saudi Arabia

<sup>10</sup>Department of Bioengineering, Department of Chemical and Biomolecular Engineering, Department of Radiology, California NanoSystems Institute (CNSI), University of California, Los Angeles, California, USA

<sup>11</sup>Department of Mechanical and Materials Engineering, University of Nebraska, Lincoln, Nebraska, USA

<sup>1</sup>Department of Medicine, Brigham and Women's Hospital, Harvard Medical School, Cambridge, Massachusetts, USA

<sup>2</sup>Harvard-MIT Division of Health Sciences and Technology, Massachusetts Institute of Technology, Cambridge, Massachusetts, USA

<sup>3</sup>Department of Civil, Chemical and Environmental Engineering (DICCA), University of Genoa, Genoa, Italy

<sup>4</sup>Department of Mechanical Engineering, Politecnico di Milano, Milan, Italy

<sup>5</sup>School of Packaging and Department of Supply Chain Management, Michigan State University, East Lansing, MI, USA

<sup>6</sup>Orthopedic Research Center, Clinical Research Unit, Mashhad University of Medical Sciences, Mashhad, Iran

<sup>7</sup>Laboratoire d'ingénierie des biomolécules (LIBio). ENSAIA-Université de Lorraine. 2 avenue de la forêt de Haye, TSA, Vandoeuvre-lès-Nancy Cedex, France

<sup>8</sup>Department of Chemical Engineering, Northeastern University, Boston, Massachusetts, USA

## Corresponding authors:

Bahar Aliakbarian, School of Packaging AND Department of Supply Chain Management, Michigan State University, East Lansing, MI 48824, USA.

Email: bahara@msu.edu

Ali Khademhosseini, California NanoSystems Institute (CNSI), University of California, Los Angeles, CA 90095, USA.

Email: khademh@ucla.edu

Ali Tamayol, University of Nebraska-Lincoln College of Engineering, 900 N 16th Street, Lincoln, NE 68588-0642, USA.

Email: atamayol@unl.edu

orderly or timely manner (generally, such wounds should heal in less than three months).<sup>1,2</sup> Examples of chronic wounds include burns and ulcers, which are typically prone to infections.<sup>3</sup> Simple infection characterized by redness around the wound area can be easily treated, but in more complicated cases it can develop into more invasive infection and sepsis, which are more severe and life threatening and burden the health-care system.<sup>4,5</sup>

Traditionally, wound dressings such as natural or synthetic bandages, cotton wool, lint and gauzes are used for wound management. Their primary function is to keep the wound dry and protected by allowing evaporation of wound exudates and preventing bacterial infection. However, it has been shown that maintaining the moisture in the wound environment accelerates the healing process.<sup>6–8</sup> Chronic wounds generate an exudate composed of a combination of growth factors and enzymes which aggravate the wound condition and should be removed efficiently to facilitate the healing process.<sup>9</sup> Therefore, it is essential to have a dressing which maintains an appropriate level of moisture while removing excessive exudate from the environment.<sup>10</sup> Hydrocolloids, alginate-based sponges and hydrogels have shown a great potential for managing the liquid content in the wound environment and have found significant applications in engineering advanced wound dressings.<sup>11–15</sup>

Hydrogels can be used as matrices to encapsulate active molecules, antibacterial agents and growth factors and provide a controlled release of these agents to prevent infections and promote the healing process.<sup>15–22</sup> Commercial hydrogel dressings usually last about one day before they dry out and need to be replaced. In addition, since commercial hydrogels act as a barrier preventing water evaporation from the wound, the use of these hydrogels might involve the risk of limiting oxygen access to the wound. Thus, the development of hydrogel dressings that remain flexible and breathable over time represents a challenge in wound management.

Another important function of wound dressings is inhibiting the growth of bacteria such as *Staphylococcus aureus* or *Staphylococcus epidermidis*, which are part of the skin flora and are commonly present in infected wounds.<sup>23</sup> This process has been so far achieved by the incorporation of antibiotics and antibacterial compounds such as silver as well as hyperbaric oxygen therapy.<sup>24,25</sup> Nanoparticles of silver (Ag) and zinc oxide (ZnO) with promising antimicrobial activity has been synthesized using environment-friendly and inexpensive process and they were successfully incorporated into antimicrobial bandages.<sup>26,28</sup> Silver salts have shown a great potential for preventing bacterial growth; however, they can significantly reduce

cellular growth and the healing rate at certain concentrations. Antibiotics that are also widely used to combat infections, if extensively used, may result in the formation of new drug-resistant pathogens.<sup>29</sup> Thus, the identification of a natural compound that can prevent bacterial growth without affecting wound healing and creating resistance in pathogens is of utmost importance.

Herbal drugs with antibacterial properties are safe, cheap and well-tolerated substitutes of those allopathic drugs.<sup>29</sup> For example, kaempferol and crocin were extracted from saffron crocus (*Crocus sativus L*) petals and were incorporated into two sets of biocompatible synthetic polymers, i.e. polyvinyl pyrrolidone and poly ethylene glycol, and agar polysaccharide for jellification.<sup>30</sup> These functionalized hydrogels showed good biocompatibility with *in vitro* cultured fibroblasts. Recently, natural antioxidants such as curcumin and *t*-resveratrol have been studied for their anti-inflammatory and antibacterial activities.<sup>31–35</sup> However, despite the recent advancements, wound management is still a challenging area particularly because of the complexity of the wound-healing process as well as patient variability.

Here, we develop an alginate-based hydrogel patch loaded with natural antioxidant compounds (curcumin and *t*-resveratrol). The hydrogel maintains excellent mechanical properties and oxygen permeability over time. While the antioxidant compounds act as bactericidal agents and improve cell proliferation. The hydrogels mechanical properties, as well as oxygen permeability and biocompatibility, are studied. The release profile of antioxidants, their cytotoxicity, bactericidal activity and *in vitro* wound healing properties were also assessed (Figure 1(a)). Results confirm that the developed hydrogel patch represents a new potential solution in the treatment of inflamed or infected wounds.

## Experimental section

### Materials

Alginic acid sodium salt from brown algae (Cat: A2033), glycerol, *t*-resveratrol, curcumin, calcium chloride (CaCl<sub>2</sub>), low gelling temperature agarose, acetic acid, methanol and acetonitrile (all HPLC grade) were purchased from Sigma-Aldrich (St. Louis, MO, USA). PrestoBlue Cell Viability Reagent was purchased from Life Technologies (California, USA). Dulbecco's Modified Eagle Medium (DMEM), fetal bovine serum (FBS), 0.05% Trypsin-EDTA (1X) and antibiotics Penicillin/Streptomycin (Pen/Strep) were purchased from Invitrogen (Carlsbad, CA, USA). Commercially available alginate-based patch (CVS

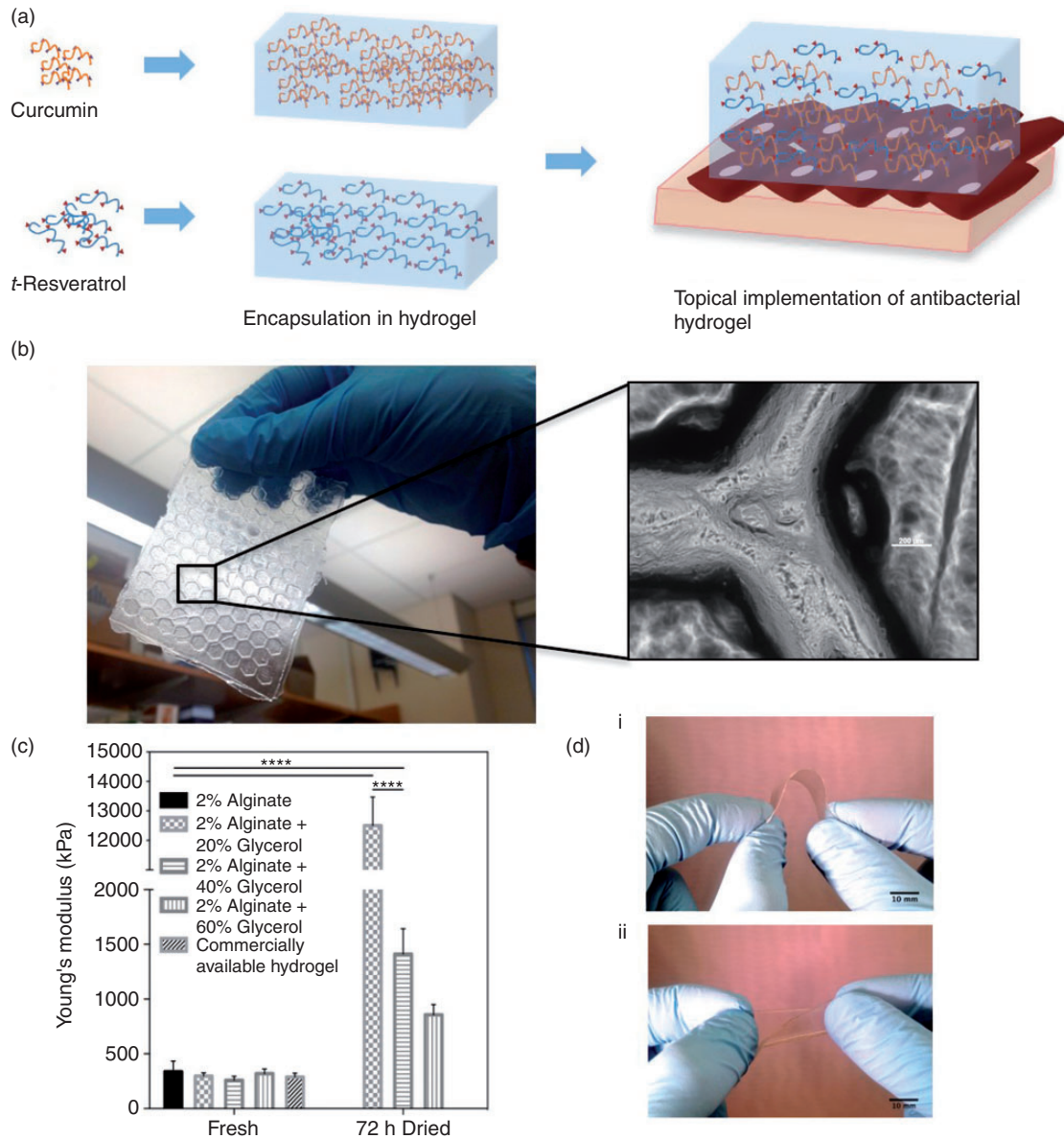


**Figure 1.** Hydrogel wound dressing for local delivery of antioxidant and antimicrobial compounds and mechanical characterization. (a) Concept of the project and its application as wound dressing. (b) A representative image of the alginate hydrogel with honeycomb structure, with the related magnification of the microchannels to facilitate air access to cells. (c) Mechanical properties of different hydrogel samples. Freshly-made samples and samples after 72 h dehydration at 37°C were compared (\*\*\*\* $p < 0.0001$ ). (d) Images showing the visual appearance and resistance of the 2% (w/v) alginate with 20% (v/v) of glycerol hydrogel after 72 h at 37°C under (i) bending and (ii) twisting (scale bar: 10 mm).

Health Sterile Hydrogel Burn Pads 4 Ct, 1.96 in  $\times$  2.95 in) was purchased from CVS pharmacy (Boston, MA, USA).

### Hydrogel preparation

Alginate-based hydrogels were fabricated with different concentrations of glycerol. Briefly, sodium alginate was dissolved in deionized water (DI) in order to prepare a stock solution with a concentration equal to 5% (w/v),

stored at 4°C. Then, the stock solution was diluted with water and glycerol in order to produce a 2% (w/v) solution of alginate. Alginate hydrogels are flexible materials, but they are prone to rapid dehydration that may lead to a brittle material. To overcome this issue, glycerol with hygroscopic properties was added to alginate to enhance the mechanical properties of the hydrogel. Four different solutions were prepared: 2% (w/v) of Na-alginate, 2% (w/v) of Na-alginate with 20% (v/v) of glycerol, 2% (w/v) of Na-alginate with

40% (v/v) of glycerol and 2% (w/v) of Na-alginate with 60% (v/v) of glycerol.

To crosslink and form the alginate hydrogels, an aqueous solution of 2% (w/v) calcium chloride ( $\text{CaCl}_2$ ) and 2% (w/v) agarose was poured in to a PDMS flat or grooved mold and left at room temperature for 30 min to solidify. The alginate solutions were poured into another PDMS mold and the agarose gel containing  $\text{CaCl}_2$  was used to cover the solution for 30 min to allow calcium diffusion and crosslinking of alginate sheets. The grooved molds would enable the fabrication of channeled hydrogel dressing, which can facilitate oxygen and exudates management.

Drug-embedded hydrogels were prepared by adding a small amount of ethanolic solution of *t*-resveratrol and curcumin in order to reach a specific concentration. Specifically, two different concentrations were assessed for both compounds: 150 and 300  $\mu\text{g}/\text{mL}$ . Concentrations of *t*-resveratrol and curcumin were chosen according to a literature review, based on the minimum concentration that is active against bacteria.<sup>36,37</sup>

### Mechanical characterization

The mechanical properties of the hydrogels were measured at room temperature using an Instron 5542 mechanical tester (Norwood, MA, USA) with a 1-kN load cell following the method used to measure the mechanical properties of GelMA and other hydrogels.<sup>38,39</sup> Briefly, samples were glued to two clamps to avoid slipping and stretched up to final rupture. Hydrogel samples were tested at a strain rate of 1 mm/min. The Young's modulus was determined as the slope of the linear region of the stress-strain curve corresponding to 10% strain. Mechanical properties of a commercially available alginate-based hydrogel were also characterized by tensile stress-strain measurement.

### Water uptake

To evaluate the performance of managing the exudate, the water uptake capacity of different alginate-with-glycerol hydrogels was measured. Samples were immersed in Dulbecco's phosphate-buffered saline (DPBS) for 3h and kept at 37°C. After removing the excess surface water, the swollen weight of each hydrogel was recorded. The water uptake was calculated as the ratio of the wet mass after 3h to the initial mass.

### Oxygen permeability

To evaluate the breathability and the oxygen permeation through the hydrogels, we designed and set up a cylindrical sealed chamber, with an inlet for the

nitrogen flow and an outlet valve to remove air from the chamber. On the opposite side, the sample's spot was designed as a two-rings structure, between which the sample was placed. Oxygen concentration was monitored using a Neofix in-situ oxygen monitoring kit with probe (Ocean Optics). After placing the sample in position, nitrogen was purged inside the changer until the oxygen concentration was equal to 0%. Then, nitrogen flow was stopped and the outlet valve was closed. A circular window ( $\text{Ø} = 35.7\text{ mm}$ ) allowed the permeation of the atmospheric air into the chamber only through the sample. The variation of the oxygen concentration was monitored over 15 min.

Different alginate-glycerol hydrogels and a commercially available alginate-based hydrogel were tested. A PDMS sheet was also tested as reference, since it is known as a gas-permeable material. All the samples had the same thickness (1 mm).

### Release studies

To check the release of biologically active compounds to the wound area, we carried out a release study using a model with air-liquid interface (ALI) in order to mimic the real conditions of loaded drug release on the wound area. *t*-Resveratrol and curcumin were chosen as biologically active compounds. Several studies have shown their activity as antioxidant, anti-inflammatory and antibacterial compounds.<sup>40</sup> Following the procedure available in the literature, a small amount of ethanolic solution of the compounds was added to the solution of alginate with 20% of glycerol before the crosslinking step, in order to have a drug concentration equal to 150 and 300  $\mu\text{g}/\text{mL}$ . Samples were placed on the ALI and release profile evaluation was performed using DPBS with 10% of ethanol (total volume 5 mL) in an incubator at 37°C. At specific time points, an aliquot of the solvent (500  $\mu\text{L}$ ) was withdrawn, frozen at -20°C and then freeze-dried. Samples were then dissolved using a small volume of ethanol and analyzed by HPLC-DAD (Hewlett Packard 1100 Series, CA, USA) equipped with a C18 reverse phase column (Vydac 201TP54, CA, USA) following the method described by Aliakbarian et al.<sup>40</sup>

### Antibacterial evaluation

To evaluate the antibacterial activity, disk diffusion test was assessed using drug-embedded hydrogels with 20% (v/v) of glycerol. *Staphylococcus aureus* which is a Gram-positive strain and the most frequent bacteria found in infected wounds was used in the experiments. Samples were cut into circular disc (6 mm of diameter, 1 mm of thickness) and normal 2% (w/v) alginate with

20% (v/v) glycerol was used as control. Samples were placed on mannitol salt agar plate and then incubated at 37°C for 24 h. If the concentration of drug was enough to reach the inhibition, a clear disk could be observed around the sample, meaning that bacteria were not able to grow or were killed in that zone.

### Cell studies

Human keratinocytes were maintained in Dulbecco's Modified Eagle Medium (DMEM, Life Technologies) supplemented with 10% FBS and 1% Pen/Strep. Cells were culture in a 5% CO<sub>2</sub> atmosphere at 37°C. Cells were passaged approximately once per week and media was exchanged every 2 days. Cells were used after ~80% confluency.

To assess the cytotoxicity or any negative impact of the hydrogel dressings on wound closure, cell viability tests were performed on human keratinocytes, which are key cells in the process of wound healing. For this study, 2% (w/v) alginate hydrogels with different concentrations of glycerol (13.4 mm × 4.3 mm × 1.5 mm L × W × T) were prepared. For drug-embedded hydrogels, a small amount of *t*-resveratrol and curcumin was added in order to have a concentration of drug equal to 150 and 300 µg/mL. Before crosslinking the alginate, all the solutions were filtered with sterile filters under biological hood (porosity: 0.22 µm). HaCaTs were then seeded with a cell density of 50 × 10<sup>3</sup> cells/mL. Samples were incubated in a 5% CO<sub>2</sub> atmosphere at 37°C and the media was changed every 24 h. Cellular metabolic activity was evaluated by PrestoBlue assay according to manufacturer protocol. The blue stain PrestoBlue reagent was uptaken by viable cells and reduced to a fluorescing stain. The extent of reduction is directly proportional to the cells' metabolic activity. The assay was performed on days 1, 3 and 7 and the fluorescent intensity was measured using a BioTek UV/vis Synergy 2 microplate reader. HaCats with the same cell density and without hydrogels were seeded and their metabolic activity were evaluated as positive blank.

To evaluate any influence of the hydrogels on cells' morphology, cells were fixed after 7 days and stained with F-Actin and DAPI to visualize actin filaments and cell nuclei, respectively. Pictures were taken using a Zeiss Axio observer D1 microscope.

For the scratch assay, keratinocytes were cultured in 24-well plates until a confluent cell layer was formed. Then a 100-µm scratch was formed using a pipette tip and drug-embedded hydrogels were placed inside culture inserts (pore size of 8 µm). Microscopic images taken over a period of 24 h to identify the migration rate of keratinocytes were analyzed using ImageJ software. The coverage percentage was evaluated by

measuring the scratch surface directly after scratching and after 24 h.

### Statistical analysis

Data are presented as mean ± standard deviation (SD). Statistical analysis was performed using GraphPad Prism 6 (San Diego, USA). Data were analyzed using one- and two-ways ANOVA multiple comparison. Statistically significant values are presented as \**p* < 0.05, \*\**p* < 0.01, \*\*\**p* < 0.001 and \*\*\*\**p* < 0.0001.

### Results

Alginate-based hydrogels were fabricated by crosslinking a mixture of 2% Na-alginate and glycerol using a flat sheet of agarose gel (2% w/v) containing CaCl<sub>2</sub> (2% w/v). The Na-alginate was crosslinked through exchanging Na<sup>+</sup> with Ca<sub>2</sub><sup>+</sup> forming a hydrophilic network of calcium alginate (Figure S1). Samples were then washed with deionized water to remove the excess of uncrosslinked polymer. This production process allowed the formation of hydrogel with a well-defined structure. Following the same procedure, we were also able to fabricate alginate patch with a high-resolution honeycomb structure. Microchannels presented on the hydrogel surface are able to guarantee a higher air and oxygen supply to the skin surface (Figure 1(b)).

Alginate hydrogels are flexible materials, but they are prone to rapid dehydration, rendering them brittle. For this reason, glycerol, which is a hygroscopic molecule and resist evaporation at room temperature, was added to alginate. The effect of different concentrations of glycerol (0–60%) on the mechanical and handling properties was assessed (Figure 1(c and d)). Properties of the obtained hydrogels were compared to a commercially available alginate-based patch (CVS Health Sterile Hydrogel Burn Pads 4 Ct, 1.96 in × 2.95 in). To investigate the lifetime of the engineered patch and simulate its operating condition, the samples were kept at 37°C for 72 h. The results showed that glycerol had no significant effect on the mechanical properties of fresh hydrogels, but its contribution became significant when the hydrogel was dried at 37°C for 72 h. After 24 h, the commercial alginate patch, as well as pristine alginate sample, was brittle and fully dried and, thus, could not withstand the tensile loading. Conversely, glycerol-containing hydrogels displayed improved mechanical properties (Figure 1(c)). Hydrogels containing only 20% (v/v) of glycerol had a 40-fold increase in their young's modulus after 72 h of drying. The change in hydrogel's young modulus was about fourfold and threefold when the glycerol concentration was 40% and 60%, respectively. This

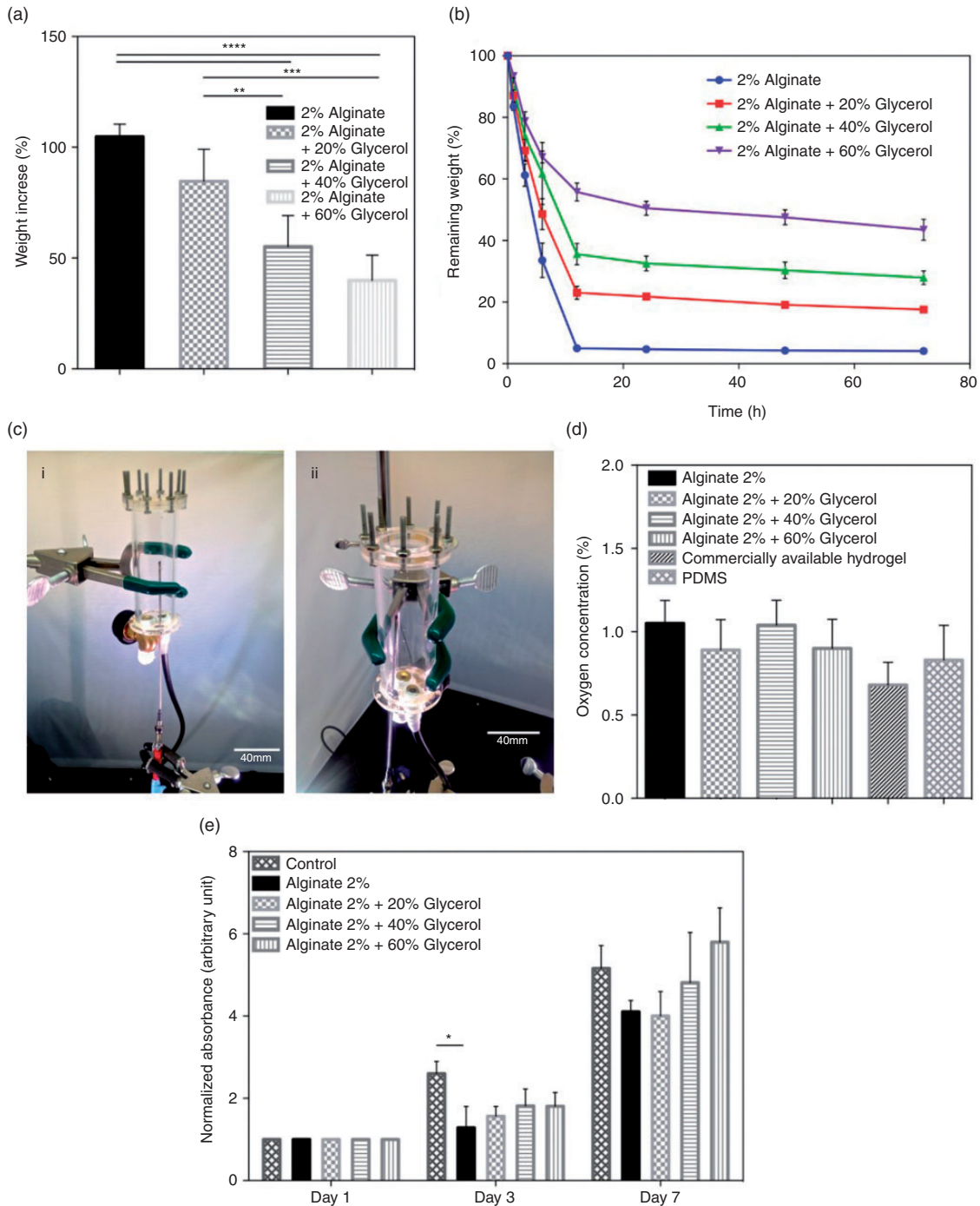


**Figure 2.** Physical characterization and biocompatibility of alginate-based hydrogels. (a) Variation of the water uptake as a function of glycerol concentration. (b) Effect of glycerol concentration (v/v) on the dehydration rate of the hydrogels. (c) Images showing the homemade chamber for the oxygen permeability test (scale bar: 40 mm). (d) Oxygen permeability as a function of the glycerol concentration, compared to a commercially available hydrogel and PDMS. (e) Metabolic activity of cells cultured with hydrogel containing different concentrations of glycerol. (\* $p < 0.05$ , \*\* $p < 0.01$ , \*\*\* $p < 0.001$  and \*\*\*\* $p < 0.0001$ ).

demonstrates the plasticizing effect of glycerol leading to the fabrication of durable flexible patches that retain their flexibility even after 27 h at 37°C (Figure 1(d)) in contrast to commercial patches which become fragile after only 10 h.

A pre-requisite of hydrogel material to be used for wound dressing purposes is the ability of managing the excessive wound exudate, particularly typical of chronic wounds. Following BS EN 13726 standard (British Standards Institution, “Test methods for primary wound

dressings. Aspects of absorbency”),<sup>41</sup> we assessed the water uptake and degradation rate of alginate hydrogels (10 × 10 mm, n = 6) with different concentrations of glycerol in 2 mL of aqueous solution of Na<sup>+</sup> (142 mmol) and Ca<sup>2+</sup> (2.5 mmol) with an ionic composition similar to human serum and wound exudate, as suggested by the standard. The results shown in Figure 2(a) indicate that after 3 h the samples absorbed exudate-mimicking solution to different extents, with the alginate sample exhibiting the highest absorption (around 100% increase in weight) and glycerol-containing samples with 45%–80% increase in weight. The liquid uptake capacity decreased for hydrogels containing higher concentrations of glycerol. This is probably caused by higher concentrations of glycerol rendering alginate-based hydrogels water impermeable, leading to a lower exudate uptake. We also evaluated the effect of glycerol on the dehydration rate of hydrogels (Figure 2(b)). Results showed a more gradual dehydration rate for glycerol-containing hydrogels in comparison to pristine alginate. Pristine alginate samples lost around 90% of their weight in less than 20 h, while glycerol-containing samples lost between 80 and 60% after 20 h of dehydration. The final remaining weight of the alginate glycerol samples was approximately 18%, 28% and 44% (for 20%, 40% and 60% v/v of glycerol, respectively), which were lower than the nominal values. We speculated that when glycerol concentration increases, the alginate network was not able to embed such amount of plasticizer and probably some was lost during the fabrication process.

Another important characteristic of wound patches is their gas permeability, especially to oxygen, since its delivery to the wound area has a key role in promoting the healing process.<sup>42</sup> Oxygen permeability of alginate samples with different concentrations of glycerol was assessed using a custom-built chamber (Figure 2(c)). Briefly, at one side the air-tight chamber had an inlet for nitrogen gas, an outlet valve and a plug for the oxygen probe. On the other side, samples were placed on a circular window, which allowed gas permeation only through the samples (Figure 2(c)). First, nitrogen was purged into the chamber, with the outlet valve opened, until all the oxygen was completely removed from inside. Then, the nitrogen flow was stopped and the oxygen concentration inside the chamber was monitored over time. The proper sealing of the platform was tested by placing an impermeable rubber and observing no significant change in oxygen concentration over time. Alginate samples were also compared to a commercially available alginate-based hydrogel and a PDMS sheet, which is known to be a gas-permeable polymer used for engineering breathable bioreactors used in cell culture.<sup>43</sup> Results showed no significant

variation among alginate-based samples ( $p < 0.05$ ) (Figure 2(d)), leading to the conclusion that the tested materials had suitable gas permeability.

The biocompatibility of fabricated hydrogels was evaluated by culturing alginate hydrogels containing different concentrations of glycerol with human immortalized keratinocytes, the predominant cell line in epidermis. Cells were cultured at the bottom of multi-well plates and samples were placed in cell culture inserts (8.0 μm pore). The metabolic activity of the cells was evaluated over the course of seven days as indicator of cell proliferation and viability (Figure 2(e)). Results suggested no significant variation in cellular activity due to the different concentration of glycerol and confirmed hydrogel biocompatibility even with high concentrations of glycerol.

Recently, engineering of wound patches with antioxidant compounds has attracted a great interest as they can modulate immune system response and can also offer antibacterial activity.<sup>44</sup> Curcumin is a derivative of o-methoxyphenol and possesses high free-radical scavenging, anti-inflammatory and antibacterial properties.<sup>45–47</sup> Resveratrol is a natural polyphenolic compound derived from grapes which also exhibits anti-bacterial properties and has shown to enhance tissue regeneration in diabetic rats.<sup>37,48–50</sup> Considering the high potential of antioxidant agents in modulating different aspects of the healing process, we added two antioxidant compounds, i.e. curcumin and *t*-resveratrol, to the alginate hydrogel. The composition of 2% (w/v) alginate with 20% (v/v) of glycerol was selected for these experiments due to its overall better characteristics. We added *t*-resveratrol and curcumin to the hydrogel matrix separately, both as ethanolic solutions, to achieve two different concentrations (150 and 300 μg/mL, respectively). Concentrations of *t*-resveratrol and curcumin were chosen according to the data available in the literature, based on the minimum concentration that was reported to be potent against bacteria.<sup>36,37</sup> First, we investigated the influence of the active compounds on the mechanical properties of the alginate hydrogel (Figure 3(a)). The obtained data showed a slight increase in the ultimate tensile strength for the sample containing 300 μg/mL of curcumin, while there was no significant difference between the samples and the hydrogel without the antioxidants. Thus, it was concluded that the suitable mechanical properties of the hydrogels were preserved after addition of the antioxidant solutions to the alginate. It is likely that the slight change observed in mechanical properties might be attributed to the ethanol rather than to the antioxidant compounds.

The engineered alginate patch was used to provide controlled release of antioxidants in order to modulate the function of immune system and prevent hyper-

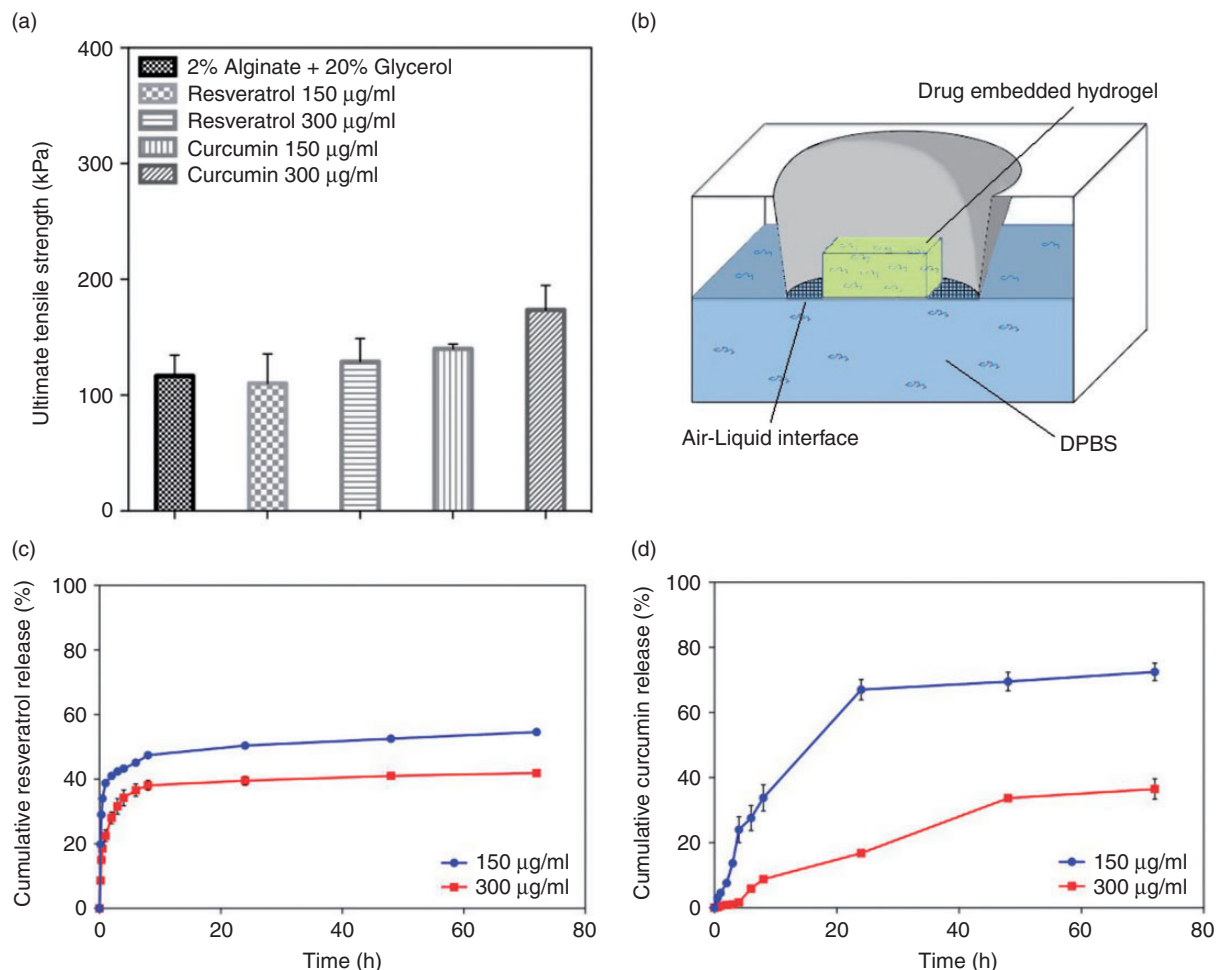


**Figure 3.** Mechanical characterization and drug release from the drug-embedded hydrogels. (a) Variation of mechanical properties of the hydrogels as a function of the concentration of the added antioxidant compound. (b) Schematic illustration of the air-liquid interface (ALI) used for drug release test. (c) Cumulative release of *t*-resveratrol from alginate hydrogel with different initial concentrations. (d) Cumulative release of curcumin from alginate hydrogel with different initial concentrations. (\*\* $p < 0.01$ , \*\*\* $p < 0.001$  and \*\*\*\* $p < 0.0001$ ).

inflammation and prevent bacterial growth. Thus, we initially evaluated the release of antioxidants through the hydrogel patch using FITC-dextran over 72 h, which is a standard molecule used to assess the release of active compounds (Figure S3). The majority of the encapsulated FITC-dextran was released within the first 24 h. To assess the release rate of active compounds from the hydrogel patches and to mimic the topical application of the patch, we formed an ALI (Figure 3(b)). In fact, the release using the ALI occurs only through one surface that will eventually be in contact with skin, thus it better simulates the final application of the engineered topical wound patch. Cumulative release of *t*-resveratrol and curcumin were evaluated at 37°C over the course of 72 h (Figure 3(c and d)) using the ALI configuration. For *t*-resveratrol, the results indicated an initial burst

release, after which the mechanism of release was governed by diffusion. After 72 h, cumulative release of 55% and 42% were measured for samples loaded with 150 and 300 µg/mL of *t*-resveratrol, respectively. Regarding curcumin, the obtained data showed a smaller burst release compared to *t*-resveratrol. Cumulative release reached 73% and 37% after 72 h for samples with 150 and 300 µg/mL of curcumin, respectively. Both the release profiles presented a shift between samples with lower and higher concentration of the drug. It is worth to notice that both the releases are expressed as percentage of cumulative release. Thus, even though the profiles of the samples with higher concentrations of drugs are lower, the actual amounts of released drugs are higher. In fact,  $\approx 8.1$  and  $\approx 12.3$  µg were released from samples with 150 and 300 µg/mL of *t*-resveratrol, respectively, while the

same amount of curcumin ( $\approx 10.8$  and  $\approx 10.8$   $\mu\text{g}$ ) was released from samples with 150 and 300  $\mu\text{g}/\text{mL}$  of curcumin, respectively. The maximum release of curcumin from the sample was reached after 72 h. This could be attributed to the lower water solubility of curcumin (3.12  $\text{mg}/\text{L}$ ) compared to *t*-resveratrol (30  $\text{mg}/\text{L}$ ). Based on the release data, we also evaluated the amount of drug released per  $\text{cm}^2$  of skin. We obtained a release of 25.0 and 40.0  $\mu\text{g}/\text{cm}^2$  for samples with 150 and 300  $\mu\text{g}/\text{mL}$  of *t*-resveratrol, respectively. Approximately, 33.3  $\mu\text{g}/\text{cm}^2$  were released for both curcumin-loaded samples.

To confirm the biocompatibility of the hydrogel patch, hydrogel samples with *t*-resveratrol and curcumin were cultured with human keratinocytes for seven days and cell metabolic activity was assessed by PrestoBlue assay (Figure 4(a)). Results suggested no negative effect on cell growth, except for the sample with higher concentration of curcumin. In this case, cells did not grow during the considered time,

suggesting a possible toxicity of curcumin at that level. This is in agreement with the previous observations of Lundvig et al.,<sup>51</sup> who reported a caspase-dependent apoptosis in HaCaT cells induced by curcumin in a dose-dependent manner. However, hydrogel with 150  $\mu\text{g}/\text{mL}$  of *t*-resveratrol seemed to improve cell growth, compared to the control samples. After seven days of culture, cells were stained with F-actin and DAPI and no visible changes were noticed on cell morphology (Figure 4(b)).

Finally, antimicrobial activity of the drug-embedded hydrogels was assessed against *S. aureus*, which is a Gram-positive bacteria and part of the typical skin flora. A qualitative analysis of antibacterial properties of hydrogels was assessed by disk diffusion method. Disks of hydrogel with different concentrations of *t*-resveratrol and curcumin were placed on an agar plate where bacteria were previously inoculated, and incubated for 24 h. After that time, formation of a circular ring around the sample, called inhibition

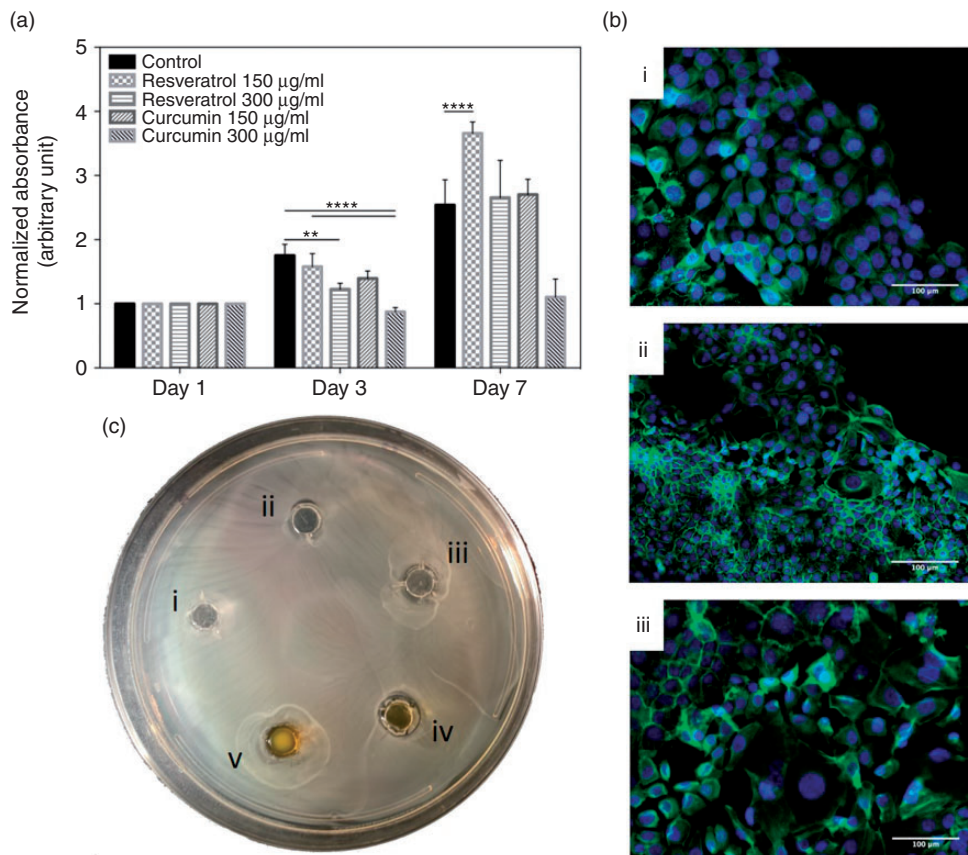


**Figure 4.** Biocompatibility and antimicrobial activity of the drug-embedded hydrogels. (a) Cell metabolic activity of keratinocytes exposed to hydrogels with different concentrations of drugs. (b) Fluorescent micrographs of F-actin (green) and DAPI (blue) staining of keratinocytes (i) control (i) and cultured with 150  $\mu\text{g}/\text{mL}$  of *t*-resveratrol (ii) and curcumin (iii). (c) Evaluation of antimicrobial activity against *Staphylococcus aureus* by disk diffusion test of alginate 2% with 20% of glycerol (i) and hydrogel with 150  $\mu\text{g}/\text{mL}$  of *t*-resveratrol (ii), 300  $\mu\text{g}/\text{mL}$  of *t*-resveratrol (iii), 150  $\mu\text{g}/\text{mL}$  of curcumin (iv) and 300  $\mu\text{g}/\text{mL}$  of curcumin (Scale bar: 100  $\mu\text{m}$ ). (\*\* $p < 0.01$  and \*\*\*\* $p < 0.0001$ ).

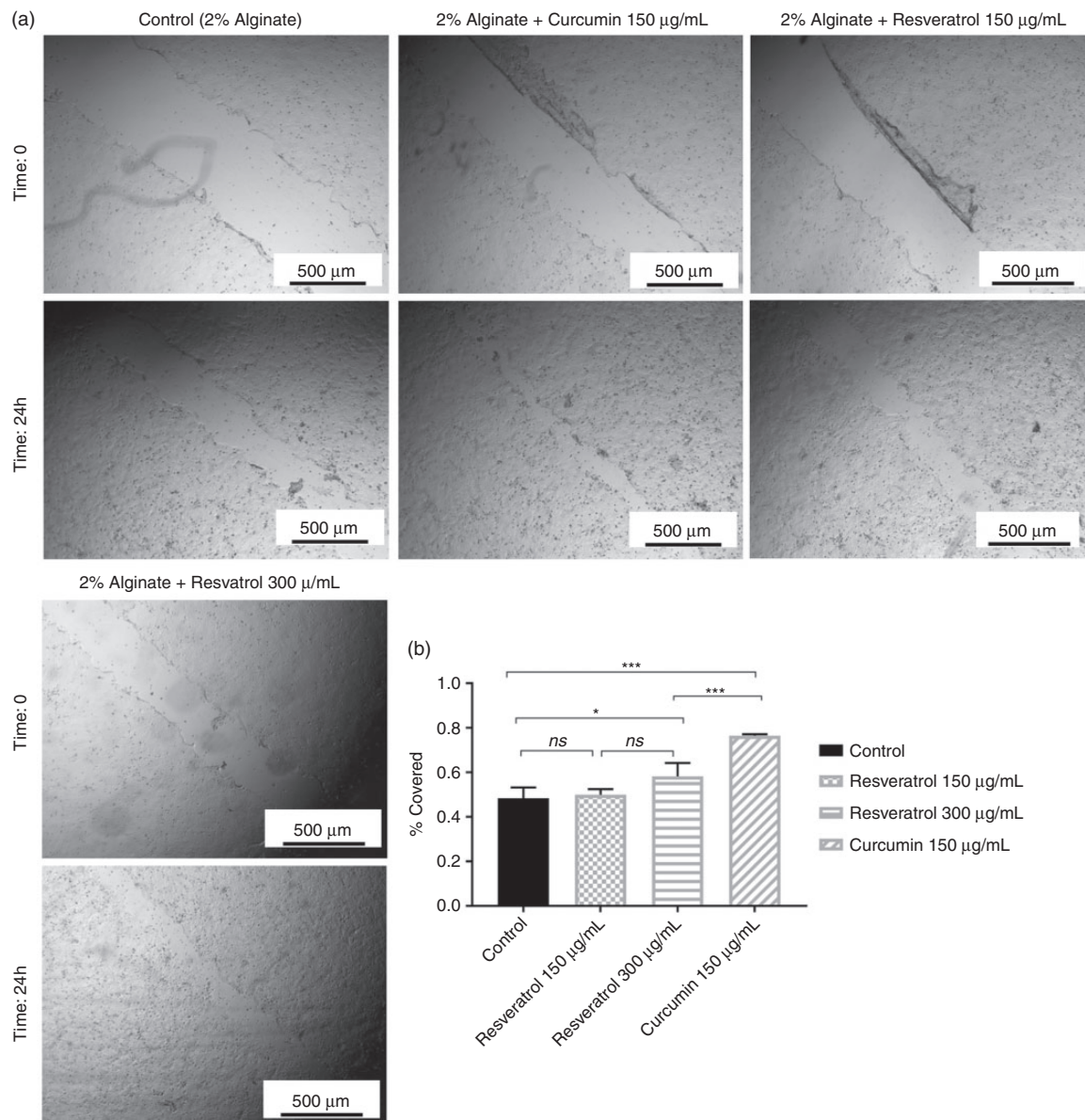


**Figure 5.** Evaluating the wound-healing properties of drug-embedded hydrogels. (a) Scratch assays carried out over samples in contact with hydrogels loaded with different concentrations of drugs. (b) Evaluating the scratch coverage percentage after 24 h contact with drug-embedded hydrogels. ( $n = 5$  for each sample,  $*p < 0.05$ ,  $**p < 0.01$ ,  $***p < 0.001$ ,  $****p < 0.0001$ ).

zone, attested the activity of the released compound against the bacteria, which are not able to grow or were killed. Results indicated that all the evaluated hydrogels were active against the considered bacteria, while the control (2% w/v alginate with 20% v/v glycerol) did not show any activity against the microbial growth (Figure 4(c)).

To assess the effectiveness of the alginate-based dressings and the released compounds in healing of skin cuts, a conventional scratch assay was conducted in which an approximately 100-µm wide scratch was created in a confluent monolayer of keratinocytes

(Figure 5). The dressings were placed on top of cell culture inserts at the ALI to release the loaded drugs into the culture media. We assessed the scratch closure after 24 h and the results suggested that only samples containing 300 µg/mL of *t*-resveratrol showed a faster closure in comparison to the negative control. On the other hand, 150 µg/mL of curcumin showed a faster scratch closure. Overall, the results suggested that curcumin offers a higher bacteriostatic effect as well as stimulatory effect for cellular growth. Combined with the well-documented anti-inflammatory effects of curcumin, we believe that alginate dressings containing

curcumin can be an excellent dressing for treatment of skin disorders. However, this yet remains to be evaluated *in vivo* using future animal studies.

## Conclusions

We fabricated an alginate-based hydrogel with embedded biologically active compounds. The developed hydrogel patch is breathable and able to maintain excellent mechanical properties over time (at least 72 h). Two antioxidants including curcumin and *t*-resveratrol were separately encapsulated within the alginate-based hydrogel and their release rate was evaluated. The results suggested a burst release followed by a gradual release of active compounds. The hydrogel was biocompatible and the antioxidants containing curcumin up to 150 µg/mL and *t*-resveratrol up to 300 µg/mL did not induce any toxicity to human keratinocytes. The patch containing curcumin was more potent against bacterial growth. The engineered wet wound dressings can be used for the treatment of many skin disorders as they can both modulate immune response and control bacterial growth.

## Declaration of Conflicting Interests

The author(s) declared no potential conflicts of interest with respect to the research, authorship, and/or publication of this article.

## Funding

The author(s) disclosed receipt of the following financial support for the research, authorship, and/or publication of this article: The author(s) received no financial support for the research, authorship, and/or publication of this article: AK and AT acknowledge funding from the National Institutes of Health (GM126831, AR073822). AT acknowledges financial support from the University of Nebraska-Lincoln and Nebraska Tobacco Settlement Biomedical Research Enhancement Funds.

## ORCID iD

Ali Tamayol  <http://orcid.org/0000-0003-1801-2889>

## References

1. Wysocki AB, Staiano-Coico L and Grinnell F. Wound fluid from chronic leg ulcers contains elevated levels of metalloproteinases MMP-2 and MMP-9. *J Invest Dermatol* 1993; 101: 64–68.
2. Tarnuzzer RW and Schultz GS. Biochemical analysis of acute and chronic wound environments. *Wound Repair Regen* 1996; 4: 321–325.
3. Tamayol A, Hassani Najafabadi A, Mostafalu P, et al. Biodegradable elastic nanofibrous platforms with integrated flexible heaters for on-demand drug delivery. *Scientific Rep* 2017; 7: 9220.
4. Koontz FP. Trends in post-operative infections by Gram-positive bacteria. *Int J Antimicrob Agents* 2000; 16: 35–37.
5. National Guideline C. Surgical site infection: prevention and treatment of surgical site infection Rockville MD: Agency for Healthcare Research and Quality (AHRQ). Retrieved from <https://www.guideline.gov/content.aspx?id=13416>.
6. Svensjo T, Pomahac B, Yao F, et al. Accelerated healing of full-thickness skin wounds in a wet environment. *Plast Reconstruct Surg* 2000; 106: 602–612. discussion 13–4.
7. Atiyeh BS, Ioannovich J, Al-Amm CA, et al. Management of acute and chronic open wounds: the importance of moist environment in optimal wound healing. *CPB* 2002; 3: 179–195.
8. Xu R, Xia H, He W, et al. Controlled water vapor transmission rate promotes wound-healing via wound re-epithelialization and contraction enhancement. *Scientific Rep* 2016; 6: 24596.
9. Saghazadeh S, Rinoldi C, Schot M, et al. Drug delivery systems and materials for wound healing applications. *Adv Drug Deliv Rev* 2018; 127: 138–166.
10. Derakhshandeh H, Kashaf SS, Aghabaglou F, et al. Smart bandages: the future of wound care. *Trend Biotechnol* 2018; 36: 1259–1274.
11. Seaman S. Dressing selection in chronic wound management. *J Am Podiatr Med Assoc* 2002; 92: 24–33.
12. Smeets R, Ulrich D, Unglaub F, et al. Effect of oxidised regenerated cellulose/collagen matrix on proteases in wound exudate of patients with chronic venous ulceration. *Int Wound J* 2008; 5: 195–203.
13. Sood A, Granick MS and Tomaselli NL. Wound dressings and comparative effectiveness data. *Adv Wound Care (New Rochelle)* 2014; 3: 511–529.
14. Dabiri G, Damstetter E and Phillips T. Choosing a wound dressing based on common wound characteristics. *Adv Wound Care (New Rochelle)* 2016; 5: 32–41.
15. Ziegler UE, Schmidt K, Keller HP, et al. Treatment of chronic wounds with an alginate dressing containing calcium zinc and manganese. *Fortschritte Der Medizin Originalien* 2003; 121: 19–26.
16. Annabi N, Rana D, Shirzaei Sani E, et al. Engineering a sprayable and elastic hydrogel adhesive with antimicrobial properties for wound healing. *Biomaterials* 2017; 139: 229–243.
17. Bagherifard S, Tamayol A, Mostafalu P, et al. Dermal patch with integrated flexible heater for on demand drug delivery. *Adv Healthcare Mater* 2016; 5: 175–184.
18. Eiselt P, Yeh J, Latvala RK, et al. Porous carriers for biomedical applications based on alginate hydrogels. *Biomaterials* 2000; 21: 1921–1927.
19. Kamata H, Li X, Chung UI, et al. Design of hydrogels for biomedical applications. *Adv Healthcare Mater* 2015; 4: 2360–2374.
20. Pal K, Banthia AK and Majumdar DK. Hydrogels for biomedical applications: a short review. *J Mater Sci Mater Med* 2014; 25: 2215.

21. Mostafalu P, Kiaee G, Giatsidis G, et al. A textile dressing for temporal and dosage controlled drug delivery. *Adv Funct Mater* 2017; 27: 1702399.
22. Faramarzi N, Yazdi IK, Nabavinia M, Gemma A, Fanelli A, Caizzone A, et al. Patient-Specific Bioinks for 3D Bioprinting of Tissue Engineering Scaffolds. *Advanced healthcare materials* 2018; 7(11): 1701347.
23. Mostafalu P, Tamayol A, Rahimi R, et al. Smart bandage for monitoring and treatment of chronic wounds. *Small* 2018; 14: 1703509.
24. Wright JB, Lam K, Buret AG, et al. Early healing events in a porcine model of contaminated wounds: effects of nanocrystalline silver on matrix metalloproteinases, cell apoptosis, and healing. *Wound Repair Regen* 2002; 10: 141–151.
25. Rattananuengsrikul V, Pimpha N and Supaphol P. In vitro efficacy and toxicology evaluation of silver nanoparticle-loaded gelatin hydrogel pads as antibacterial wound dressings. *J Appl Polym Sci* 2012; 124: 1668–1682.
26. Khatami M, Varma RS, Zafarnia N, et al. Applications of green synthesized Ag, ZnO and Ag/ZnO nanoparticles for making clinical antimicrobial wound-healing bandages. *Sustain Chem Pharm* 2018; 10: 9–15.
27. Nasajpour A, Ansari S, Rinoldi C, et al. A multifunctional polymeric periodontal membrane with osteogenic and antibacterial characteristics. *Adv Funct Mater* 2018; 28: 1703437.
28. Nasajpour A, Mandla S, Shree S, et al. Nanostructured fibrous membranes with rose spike-like architecture. *Nano Lett* 2017; 17: 6235–6240.
29. Qureshi M, Khatoon F and Ahmed S. An overview on wounds, their issues and natural remedies for wound healing. *Biochem Physiol* 2015; 4: 1453–1460.
30. Zeka K, Ruparelia KC, Sansone C, et al. New hydrogels enriched with antioxidants from saffron crocus can find applications in wound treatment and/or beautification. *Skin Pharmacol Physiol* 2018; 31: 95–98.
31. Palmieri D, Aliakbarian B, Casazza AA, et al. Effects of polyphenol extract from olive pomace on anoxia-induced endothelial dysfunction. *Microvasc Res* 2012; 83: 281–289.
32. Ferrari PF, Palmieri D, Casazza AA, et al. TNF $\alpha$ -induced endothelial activation is counteracted by polyphenol extract from UV-stressed cyanobacterium *Arthrospira platensis*. *Med Chem Res* 2014; 24: 275–282.
33. Chan MM. Antimicrobial effect of resveratrol on dermatophytes and bacterial pathogens of the skin. *Biochem Pharmacol* 2002; 63: 99–104.
34. Paulo L, Oleastro M, Gallardo E, et al. Antimicrobial properties of resveratrol: a review. *Science against microbial pathogens: communicating current research and technological advances*. 2011, pp.1225-1235.
35. De R, Kundu P, Swarnakar S, et al. Antimicrobial activity of curcumin against *Helicobacter pylori* isolates from India and during infections in mice. *Antimicrobial Agents Chemother* 2009; 53: 1592–1597.
36. Mun SH, Joung DK, Kim YS, et al. Synergistic antibacterial effect of curcumin against methicillin-resistant *Staphylococcus aureus*. *Phytomedicine* 2013; 20: 714–718.
37. Chan MM-Y. Antimicrobial effect of resveratrol on dermatophytes and bacterial pathogens of the skin. *Biochem Pharmacol* 2002; 63: 99–104.
38. Chen Y-C, Lin R-Z, Qi H, et al. Functional human vascular network generated in photocrosslinkable gelatin methacrylate hydrogels. *Adv Funct Mater* 2012; 22: 2027–2039.
39. Annabi N, Tsang K, Mithieux SM, et al. Highly elastic micropatterned hydrogel for engineering functional cardiac tissue. *Adv Funct Mater* 2013; 23. DOI: 10.1002/adfm.201300570.
40. Aliakbarian B, Casazza AA and Perego P. Valorization of olive oil solid waste using high pressure–high temperature reactor. *Food Chem* 2011; 128: 704–710.
41. Lee G, Anand SC, Rajendran S, et al. Efficacy of commercial dressings in managing malodorous wounds. *Br J Nurs* 2007; 16: S8–S20.
42. Gordillo GM and Sen CK. Revisiting the essential role of oxygen in wound healing. *Am J Surg* 2003; 186: 259–263.
43. Mehta G, Mehta K, Sud D, et al. Quantitative measurement and control of oxygen levels in microfluidic poly (dimethylsiloxane) bioreactors during cell culture. *Biomed Microdev* 2007; 9: 123–134.
44. Gupta A, Upadhyay NK, Sawhney RC, et al. A polyherbal formulation accelerates normal and impaired diabetic wound healing. *Wound Repair Regen* 2008; 16: 784–790.
45. Gopinath D, Ahmed MR, Gomathi K, et al. Dermal wound healing processes with curcumin incorporated collagen films. *Biomaterials* 2004; 25: 1911–1917.
46. Kant V, Gopal A, Pathak NN, et al. Antioxidant and anti-inflammatory potential of curcumin accelerated the cutaneous wound healing in streptozotocin-induced diabetic rats. *Int Immunopharmacol* 2014; 20: 322–330.
47. Maheshwari RK, Singh AK, Gaddipati J, et al. Multiple biological activities of curcumin: a short review. *Life Sci* 2006; 78: 2081–2087.
48. Bashmakov YK, Assaad-Khalil S and Petyaev IM. Resveratrol may be beneficial in treatment of diabetic foot syndrome. *Med Hypotheses* 2011; 77: 364–367.
49. Gokce EH, Tuncay Tanriverdi S, Eroglu I, et al. Wound healing effects of collagen-laminin dermal matrix impregnated with resveratrol loaded hyaluronic acid-DPPC microparticles in diabetic rats. *Eur J Pharmaceut Biopharmaceut* 2017; 119: 17–27.
50. Mukherjee S, Dudley JI and Das DK. Dose-dependency of resveratrol in providing health benefits. *Dose Response* 2010; 8: 478–500.
51. Lundvig DMS, Pennings SWC, Brouwer KM, et al. Cytoprotective responses in HaCaT keratinocytes exposed to high doses of curcumin. *Exp Cell Res* 2015; 336: 298–307.